

## LEAST-SQUARES FINITE ELEMENTS FOR FLUID FLOW AND TRANSPORT

G. F. CAREY,\* A. I. PEHLIVANOV, Y. SHEN, A. BOSE AND K. C. WANG

*Department of Aerospace Engineering and Engineering Mechanics, University of Texas at Austin, Austin, TX 78712, U.S.A.*

### SUMMARY

The least-squares mixed finite element method is concisely described and supporting error estimates and computational results for linear elliptic (steady diffusion) problems are briefly summarized. The extension to the stationary Navier–Stokes problems for Newtonian, generalized Newtonian and viscoelastic fluids is then considered. Results of numerical studies are presented for the driven cavity problem and for a stick–slip problem. © 1998 John Wiley & Sons, Ltd.

*Int. J. Numer. Meth. Fluids*, **27**: 97–107 (1998)

KEY WORDS: least-squares; finite elements; flow; transport

### 1. INTRODUCTION

Least-squares schemes for approximating the solution to differential equations were proposed some time ago as a particular variant of the method of weighted residuals (see, e.g. References 1 and 2). The basic idea is quite straightforward. Given a trial solution expansion with unknown coefficients and satisfying the boundary conditions, construct the corresponding residual for the differential equation. Next, minimize the integral mean square residual to generate an algebraic system. Finally, solve this algebraic system to determine the coefficients and hence the approximation. This approach is appealing because the resulting algebraic system has symmetric structure even for non-self-adjoint PDEs such as those frequently encountered in fluid flow and transport. The method is also less sensitive to changes in PDE type and for this reason was investigated in exploratory finite element studies of mixed-type problems for the Tricomi equation and subsonic/transonic flows.<sup>3,4</sup> The main detractors of this method are also clear from these studies—since the least-squares functional is constructed for the second-order operator, second-order derivatives should be square-integrable and this imposes increased smoothness requirements on the finite element spaces. For example,  $C^1$  bases are sufficient and were used in the study cited above.<sup>3</sup> This implies a high- $p$  approximation scheme which will generate accurate approximations and is topical in view of the current interest in high- $p$  methods. However, it is still generally regarded as too restrictive and particularly unappealing in 3D. Another problem is the degradation in conditioning as compared with Galerkin finite element

---

\* Correspondence to: G. F. Carey, Department of Aerospace Engineering and Engineering Mechanics, University of Texas at Austin, Austin, TX 78712, U.S.A.

systems. Applying the least-squares approach directly to the operator is somewhat analogous to applying least-squares to an algebraic system, thereby generating the symmetric normal system form. The conditioning of the system is also squared and the iterative convergence will be degraded. For these reasons the least-squares approach has received relatively little attention until recently.

The above continuity requirements can be relaxed by introducing new flux variables to recast the higher-order problem as a lower-order system. For example, a scalar potential equation for  $u$  would be replaced by a first-order system for  $u$  and flux  $\sigma$ . Now the least-squares residual functional can be formed for the system and the approximations  $(u_h, \sigma_h)$  to  $(u, \sigma)$  can be determined in the manner suggested above. In essence, we have thereby constructed a mixed least-squares finite element formulation analogous to the corresponding mixed Galerkin formulation. There are, however, two striking distinctions: (i) the least-squares system is symmetric positive whereas the Galerkin system is not; (ii) the finite element bases for the least-squares scheme are not subject to the restrictive inf-sup conditions of the Galerkin mixed methods.<sup>5</sup> Of course, as with other mixed methods, additional flux variables are introduced. The previous conditioning problems are alleviated, but the system size is still large owing to the additional flux variables. Preconditioning is still desirable and multigrid schemes have been shown to be effective (see Reference 6). Another strategy that can be interpreted as a preconditioning is to introduce a Sobolev gradient to accelerate steepest descent iteration.<sup>7,8</sup>

In the present work we focus on fluid flow and transport problems where mixed methods are gaining popularity and least-squares shows considerable promise. In particular, we develop the method for stationary elliptic problems associated with convection–diffusion and viscous Newtonian or non-Newtonian flows. However, we also include a number of reference citations to our own work and that of others dealing with the transient least-squares problem. We begin in Section 2 with a simple 1D example to introduce the methodology and state the main estimates. Then the extension to two- and three-dimensional potential problems is presented and some interesting theoretical and computational results are summarized. A brief description and results using a specific preconditioning strategy are included. Also, error estimates in subdomains are given. In Section 3 we describe the residual-based error estimator, which is exact on each finite element in the norm defined by the bilinear form. Next, in Section 4 the extension of the least-squares method to stationary viscous flows governed by the Stokes and Navier–Stokes equations is given, together with numerical results. Results for both  $h$ - and  $p$ -type finite elements have been computed. Finally, we consider the least-squares formulation for viscoelastic problems.

## 2. STEADY POTENTIAL FLOW AND TRANSPORT

The main ideas can be most conveniently introduced by means of a two-point boundary value problem for steady 1D transport. Accordingly, let us consider

$$-(au')' + cu = f, \quad 0 \leq x \leq 1, \quad (1)$$

with  $u(0) = 0$  and  $a(1)u'(1) = 0$ . Introducing the flux  $\sigma = -au'$ , we obtain the first-order system

$$\sigma' + cu = f, \quad \sigma + au' = 0, \quad (2)$$

with  $u(0) = 0$  and  $\sigma(1) = 0$ .

The corresponding least-squares functional is

$$I(u, \sigma) = \int_0^1 [(\sigma' + cu - f)^2 + (\sigma + au')^2] dx \quad (3)$$

and taking variations we get the weak statement: find  $(u, \sigma)$  satisfying the boundary conditions and such that

$$a(u, \sigma; v, q) = (f, q' + cv), \quad (4)$$

where  $(f, q' + cv)$  is the standard  $L^2$  inner product and the bilinear form

$$a(u, \sigma; v, q) = \int_0^1 [(\sigma' + cu)(q' + cv) + (\sigma + au')(q + av')] dx \quad (5)$$

is coercive in the associated space.

Existence of a unique solution then follows from the Lax–Milgram lemma and we have proven global estimates of the form<sup>9</sup>

$$\|u - u_h\|_m + \|\sigma - \sigma_h\|_m \leq Ch^{s+1-m} (\|u\|_{s+1} + \|\sigma\|_{s+1}), \quad m = 0, 1, \quad (6)$$

for  $s = \min(k, r)$  and  $C^0$  finite element spaces of degree  $k$  and  $r$  for  $u_h$  and  $\sigma_h$ , respectively. Improved estimates have been obtained for the case where  $k \neq r$  and superconvergence estimates have also been proved and numerically demonstrated.<sup>9,10</sup> For example, if  $k = r$ , the rate of convergence at the inter-element nodes is  $O(h^{2k})$  for both  $u$  and  $\sigma$ .

Let us now consider the direct extension of this formulation to the steady convection–diffusion problem in two- or three-dimensional domains  $\Omega$  defined by

$$-\nabla \cdot (a\nabla u) - \mathbf{b} \cdot \nabla u + cu = f \quad \text{in } \Omega, \quad (7)$$

with  $u = 0$  on  $\partial\Omega$ . The first-order system is then, similarly,

$$\nabla \cdot \boldsymbol{\sigma} + \mathbf{b} \cdot a^{-1} \boldsymbol{\sigma} + cu = f, \quad (8)$$

$$\boldsymbol{\sigma} + a\nabla u = \mathbf{0} \quad (9)$$

and the least-squares functional becomes

$$I(u, \boldsymbol{\sigma}) = \int_{\Omega} [(\nabla \cdot \boldsymbol{\sigma} + \mathbf{b} \cdot a^{-1} \boldsymbol{\sigma} + cu - f)^2 + (\boldsymbol{\sigma} + a\nabla u)^2] dx dy. \quad (10)$$

Error estimates for this formulation are given in References 5 and 11 (see also Reference 12). An improved result for the flux can be obtained by adding an additional curl relation

$$\nabla \times (a^{-1} \boldsymbol{\sigma}) = 0 \quad \text{in } \Omega \quad (11)$$

and boundary relation

$$\mathbf{n} \wedge (a^{-1} \boldsymbol{\sigma}) = 0 \quad \text{in } \partial\Omega, \quad (12)$$

where  $\mathbf{n}$  is the unit outward normal and  $\wedge$  denotes the exterior product. The effect of these additional terms is to produce a modified bilinear form that is coercive on a ‘better’ space and we get improved global estimates<sup>11,13</sup> of the form (for  $k = r$ )

$$\|u - u_h\|_0 + \|\boldsymbol{\sigma} - \boldsymbol{\sigma}_h\|_0 \leq Ch^{k+1} (\|u\|_{k+1} + \|\boldsymbol{\sigma}\|_{k+1}). \quad (13)$$

Numerical experiments are presented in Tables I and II for problem (8), (9) with  $a = (y^2 + 1)$ ,  $\mathbf{b} = (x, y)$ ,  $c = (5x + y)^2 + 1$  and exact solution  $u = \exp(2x^2 + 2y^2)$  on a square domain with corners  $(0, -1)$ ,  $(1, 0)$ ,  $(0, 1)$  and  $(-1, 0)$ . It is evident from Table II that the numerical rates of convergence in the usual norms are suboptimal for the case where the additional curl and boundary relations are omitted.

The least-squares mixed system conditioning depends asymptotically on the mesh size in a manner similar to the Galerkin method. As the mesh is refined, the condition number deteriorates with order

Table I. Convergence rates for case with curl term and  $\sigma_h$  boundary condition

Norm	$k = 1$	$k = 1$	$k = 2$	$k = 2$	$k = 3$
	$r = 1$	$r = 2$	$r = 2$	$r = 3$	$r = 3$
$\ u - u_h\ _0$	1.85	2.02	3.31	3.01	4.24
$ u - u_h _1$	1.08	1.01	2.16	2.00	3.14
$\ \sigma - \sigma_h\ _0$	1.91	2.10	3.01	3.89	3.99
$ \sigma - \sigma_h _1$	1.00	1.93	1.98	2.94	2.98
$\ \nabla \cdot (\sigma - \sigma_h)\ _0$	1.01	1.95	1.98	2.95	2.97

Table II. Convergence rates for case without curl term and  $\sigma_h$  boundary condition

Norm	$k = 1$	$k = 1$	$k = 2$	$k = 2$	$k = 3$
	$r = 1$	$r = 2$	$r = 2$	$r = 3$	$r = 3$
$\ u - u_h\ _0$	1.86	2.02	3.31	3.01	4.21
$ u - u_h _1$	1.08	1.01	2.14	2.00	3.12
$\ \sigma - \sigma_h\ _0$	1.07	1.73	1.95	2.36	3.11
$ \sigma - \sigma_h _1$	0.54	0.65	0.94	1.33	2.25
$\ \nabla \cdot (\sigma - \sigma_h)\ _0$	1.00	2.02	1.98	2.88	2.97

$O(h^{-2})$ . In Reference 6 we investigate the use of a block ILU scheme from Reference 14 as a preconditioner for conjugate gradient solution of the symmetric positive block least-squares system. This scheme can also be viewed as a two-grid multigrid scheme applied to the associated reduced Schur matrix with restriction to a lower-dimensional space of fixed size  $m$ . The performance of this preconditioning strategy is indicated in Table III for the above-mentioned test problem. In the table,  $m$  is the block size for the restriction operator to the lower-dimensional space and  $h = 1/n$  is the mesh size. The large block sizes require progressively more CPU time per iteration as  $m$  increases but fewer iterations to converge and are more efficient. If the curl relation and flux boundary relation are removed, the number of iterations increases. We also applied this preconditioner to problems with discontinuous diffusion coefficients. The number of iterations appears to be independent of the jump in the diffusion coefficient when proper weight is used in the curl term (see also References 6 and 15).

Estimate (13) suggests that we need to have a smooth solution to our problem in order to obtain optimal rates of convergence. In general, we cannot expect such regularity globally. However, we have sufficient smoothness in regions away from the sources of singularity. Let  $\Omega_0$  and  $\Omega_1$  be

Table III. Number of iterations for the block preconditioner

$n$	$m = 1$	$m = 2$	$m = 4$	$m = 8$
80	99	76	55	36
40	52	40	29	19
20	27	21	16	11
10	15	12	9	7

compact subdomains of  $\Omega$  with smooth boundaries. Then the following interior estimate holds (for  $k=r$ ):

$$\begin{aligned} \|u - u_h\|_{0,\Omega_0} + \|\boldsymbol{\sigma} - \boldsymbol{\sigma}_h\|_{0,\Omega_0} &\leq Ch^2(\|u - u_h\|_{1,\Omega_1} + \|\boldsymbol{\sigma} - \boldsymbol{\sigma}_h\|_{1,\Omega_1}) \\ &\quad + C(\|u - u_h\|_{1,\Omega_1} + \|\boldsymbol{\sigma} - \boldsymbol{\sigma}_h\|_{1,\Omega_1}) + Ch^{k+1}(\|u\|_{k+1,\Omega_1} + \|\boldsymbol{\sigma}\|_{k+1,\Omega_1}). \end{aligned}$$

See Reference 16 for other interior estimates, including the case of differing polynomial degrees. The above error estimate indicates that the rate of convergence on  $\Omega_0$  is controlled by the error in a weaker norm on  $\Omega_1$ .

### 3. ERROR ESTIMATOR

One of the main advantages of the least-squares mixed formulation is that we can calculate exactly the error in the norm defined by the bilinear form. Moreover, we can calculate exactly the error in this ‘energy’ norm not only globally but also on each finite element.

The discrete variational problem which corresponds to problem (8), (9) is

$$a(u_h, \boldsymbol{\sigma}_h; v_h, \mathbf{q}_h) = (f, \nabla \cdot \mathbf{q}_h + \mathbf{b} \cdot a^{-1} \mathbf{q}_h + cv_h) \quad (14)$$

for all  $v_h \in V_h$  and  $\mathbf{q}_h \in \mathbf{W}_h$ , where  $V_h$  and  $\mathbf{W}_h$  are the finite element spaces for  $u_h$  and  $\boldsymbol{\sigma}_h$ , respectively and

$$a(u_h, \boldsymbol{\sigma}_h; v_h, \mathbf{q}_h) = (\nabla \cdot \boldsymbol{\sigma}_h + \mathbf{b} \cdot a^{-1} \boldsymbol{\sigma}_h + cu_h, \nabla \cdot \mathbf{q}_h + \mathbf{b} \cdot a^{-1} \mathbf{q}_h + cv_h) + (\boldsymbol{\sigma}_h + a\nabla u_h, \mathbf{q}_h + a\nabla v_h).$$

For the error in the energy norm we have

$$\begin{aligned} a(u - u_h, \boldsymbol{\sigma} - \boldsymbol{\sigma}_h; u - u_h, \boldsymbol{\sigma} - \boldsymbol{\sigma}_h) &= (\nabla \cdot (\boldsymbol{\sigma} - \boldsymbol{\sigma}_h) + \mathbf{b} \cdot a^{-1} (\boldsymbol{\sigma} - \boldsymbol{\sigma}_h) + c(u - u_h), \\ &\quad \nabla \cdot (\boldsymbol{\sigma} - \boldsymbol{\sigma}_h) + \mathbf{b} \cdot a^{-1} (\boldsymbol{\sigma} - \boldsymbol{\sigma}_h) + c(u - u_h)) \\ &\quad + (\boldsymbol{\sigma} - \boldsymbol{\sigma}_h + a\nabla(u - u_h), \boldsymbol{\sigma} - \boldsymbol{\sigma}_h + a\nabla(u - u_h)) \\ &= (f - \nabla \cdot \boldsymbol{\sigma}_h - \mathbf{b} \cdot a^{-1} \boldsymbol{\sigma}_h - cu_h, f - \nabla \cdot \boldsymbol{\sigma}_h - \mathbf{b} \cdot a^{-1} \boldsymbol{\sigma}_h - cu_h) \\ &\quad + (\boldsymbol{\sigma}_h + a\nabla u_h, \boldsymbol{\sigma}_h + a\nabla u_h), \end{aligned} \quad (15)$$

where (8) and (9) were used at the last step. Since the right-hand side of (15) involves only  $u_h$  and  $\boldsymbol{\sigma}_h$ , we can calculate exactly the error in the ‘energy’ norm. The same argument as in (15) may be applied to any element of the finite element partition, i.e. we have an exact error estimator locally on each finite element. We tested an  $h$ -adaptive procedure based on this estimator. The numerical experiments indicate that optimal rates of convergence with respect to the number of degrees of freedom can be achieved.<sup>17</sup>

### 4. VISCOUS FLOW

Let us begin with the stationary Navier–Stokes equations in primitive variable form:

$$\mathbf{u} \cdot \nabla \mathbf{u} + \frac{1}{\rho} \nabla p - \nu \Delta \mathbf{u} = \mathbf{f}, \quad \nabla \cdot \mathbf{u} = 0. \quad (16)$$

For two-dimensional flow we may introduce the scalar vorticity field  $\zeta$  to recast (16) as the first-order system

$$\begin{aligned} u \frac{\partial u}{\partial x} + v \frac{\partial u}{\partial y} + \frac{1}{\rho} \frac{\partial p}{\partial x} + v \frac{\partial \zeta}{\partial y} &= f, & u \frac{\partial v}{\partial x} + v \frac{\partial v}{\partial y} + \frac{1}{\rho} \frac{\partial p}{\partial y} - v \frac{\partial \zeta}{\partial x} &= g, \\ \zeta - \frac{\partial v}{\partial x} + \frac{\partial u}{\partial y} &= 0, & \frac{\partial u}{\partial x} + \frac{\partial v}{\partial y} &= 0, \end{aligned} \quad (17)$$

with appropriate boundary conditions specified on  $\partial\Omega$ .

Introducing the residual vector  $\mathbf{r}$  of equations (17), the least-squares functional for admissible  $u$ ,  $v$ ,  $p$  and  $\zeta$  follows as

$$I = \int_{\Omega} \mathbf{r}^T \mathbf{r} dx dy. \quad (18)$$

Taking variations leads to a weak statement for the least-squares formulation and introducing the finite element spaces we obtain a non-linear algebraic system to be solved for the nodal solution values. For the case of slow flow, the inertial terms  $\mathbf{u} \cdot \nabla \mathbf{u}$  in (16) and (17) are negligible and the problem simplifies to Stokes flow. Then the system (17) is linear and the bilinear functional resulting from (18) is symmetric positive.

In turn, this implies that the usual consistency conditions associated with the Galerkin approach do not have to be enforced in the least-squares mixed formulation. For example, it is well known that the mixed Galerkin finite element method for the primitive variable Navier–Stokes formulation is not stable for certain equal-order basis combinations, ‘locking’ to  $\mathbf{u}_h = 0$  occurs for the linear velocity, constant pressure triangle and spurious pressure modes can occur for other choices of bases.<sup>18</sup> These restrictions on the bases do not apply to the least-squares mixed finite element formulation. Consequently, in the results presented later we use equal-order bases for all variables for convenience (although other choices are possible and may be preferable for other reasons such as computational efficiency or the requirements of a specific application).

We would also like to emphasize that there are implicit questions of scaling that arise in least-squares formulations. For instance, different physical parameters appear in different equations and scale different terms of an equation. Hence the respective residuals in the least-squares functional (18) may be differently scaled. Since the approximation minimizes  $I$  on the subspace and  $I$  is a sum of equation residuals, the accuracy of the approximation to, for instance, mass balance versus momentum balance may be difficult. This can also have some bearing on numerical scaling of the resulting algebraic system. To illustrate this point, note that the first pair of equations in (17) can be scaled by  $v^{-1}$  to rewrite the momentum equations with the inertial terms scaled by an effective Reynolds number  $Re \sim v^{-1}$ . Then, if the velocity components are scaled to be  $O(1)$  and the flow is slow so that  $Re < 1$ , the coefficients in the scaled equation are less than unity and all residuals in the functional  $I$  will have coefficients of similar order. On the other hand, the form shown in (17) might fare better numerically as the Reynolds number increases. Of course, if the mesh size is sufficiently small, either formulation would give accurate results, but from a practical standpoint we seek accurate results on the coarsest admissible grid. This issue does raise the question of weighting individual residuals in  $I$  differently. This is a topic of continuing study.

Numerical results for the formulation in (17) have been computed for the familiar lid-driven cavity problem on a  $25 \times 25$  mesh using nine-node biquadratic elements for all four solution variables. The streamfunction contours computed from  $u$  and  $v$  are shown in Figure 1(a) and the vorticity contours in Figure 1(b).

We remark that our first calculations of viscous flows date from around 1988 and appeared in Reference 19. However, we have delayed communicating subsequent computations because the

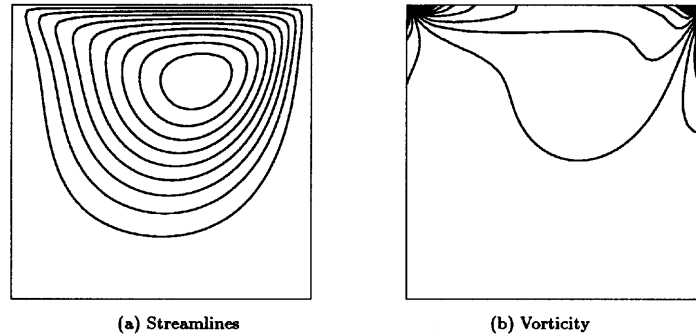


Figure 1. Solutions from velocity–pressure–vorticity scheme ( $Re = 100$ )

methods do exhibit some anomalous behaviour and warrant further study. For example, as suggested above, scaling can be an issue and we have observed that the methods applied to (17) may not demonstrate an adequate approximation to mass conservation for calculations on coarse grids at low  $Re$ . Further details and supporting numerical studies are given in Reference 20. Other related results are reported in References 21 and 22. However, using the alternative formulation at low  $Re$  has been shown to generate approximations with better mass conservation properties.

There are other formulations of the viscous flow problem that can be recast in a form suitable for least-squares treatment. Here, for brevity, we will restrict our attention to the stress formulation because of its broader applicability to generalized newtonian and viscoelastic flow problems which we also take up later. Let us first consider the stress formulation for stationary Navier–Stokes. Instead of (17) we now have

$$\begin{aligned} \rho \left( u \frac{\partial u}{\partial x} + v \frac{\partial u}{\partial y} \right) + \frac{\partial p}{\partial x} - \left( \frac{\partial \tau_{xx}}{\partial x} + \frac{\partial \tau_{xy}}{\partial y} \right) &= f, \\ \rho \left( u \frac{\partial v}{\partial x} + v \frac{\partial v}{\partial y} \right) + \frac{\partial p}{\partial y} - \left( \frac{\partial \tau_{xy}}{\partial x} + \frac{\partial \tau_{yy}}{\partial y} \right) &= g, \\ \frac{\partial u}{\partial x} + \frac{\partial v}{\partial y} &= 0, \end{aligned} \tag{19}$$

with the constitutive (Stokes) relation

$$\tau_{ij} - \eta(u_{i,j} + u_{j,i}) = 0 \tag{20}$$

for the stress tensor to complete a full system of six equations for  $u, v, p, \tau_{xx}, \tau_{xy}$  and  $\tau_{yy}$ . Note that we have replaced the kinematic viscosity  $\nu$  with the viscosity  $\eta$ . Generalized Newtonian fluids such as power-law and Bingham constitutive models can be treated by appropriately specifying  $\eta$  in (20). For example, in the power-law model we set

$$\eta = K \dot{\gamma}^{*(n-1)}, \tag{21}$$

where the constants  $K$  and  $n$  are referred to as the consistency parameter and power-law index respectively and the scalar quantity  $\dot{\gamma}^*$  is the second invariant of the shear rate tensor  $\dot{\gamma}_{ij} = (u_{i,j} + u_{j,i})$ .

Similarly, for the Bingham model we have

$$\begin{aligned} \eta &= \eta_0 + \tau_0 / \dot{\gamma}^* \quad \text{when } \frac{1}{2} \text{tr}(\boldsymbol{\tau}^2) \geq \tau_0^2, \\ \dot{\boldsymbol{\gamma}} &= \mathbf{0} \quad \text{when } \frac{1}{2} \text{tr}(\boldsymbol{\tau}^2) < \tau_0^2, \end{aligned} \tag{22}$$

where  $\eta_0$  is the Newtonian viscosity and the yield stress of the fluid material is denoted by  $\tau_0$ .

Expanding each of the six fields ( $u$ ,  $v$ ,  $p$ ,  $\tau_{xx}$ ,  $\tau_{xy}$  and  $\tau_{yy}$ ) in the finite element basis, substituting in the least-squares functional for (19) and (20) and minimizing yields a non-linear coupled system for the nodal velocity, pressure and stress components. The large number of degrees of freedom obviously implies that the resulting algebraic systems are large and these problems are both difficult and computationally intensive. However, this is true for both the Galerkin and least-squares formulations. The fact that the LBB condition must be enforced in the Galerkin finite element method is a key consideration now since it implies that the stress field approximation must be in a higher-dimensional subspace.<sup>23</sup> This is not the case with the least-squares mixed method, but scaling is still an issue.

We have computed the equal-order bilinear and biquadratic approximations and higher- $p$  approximate solutions for several test problems and different choices of fluid types. Contours of the shear stress component  $\tau_{xy}$  and vorticity for a Newtonian fluid ( $n=1$ ) and the cavity problem at  $Re=1$  with polynomial degree two on a  $20 \times 20$  uniform mesh are given in Figure 2(a).

Numerical results with an equal-order basis of polynomial degree six on a  $5 \times 5$  mesh for a power-law fluid with index  $n=0.85$  are given in Figure 2(b). An example of a Bingham fluid on a non-uniform mesh with variable local polynomial orders is shown in Figure 3(b). As the Bingham number  $Bn = \tau_0 L / \eta v_0$  is increased, more and more of the fluid in the cavity behaves like a solid and the flow is increasingly confined to near the moving wall. Various scaling issues related to least-squares minimization for Bingham fluids are discussed in Reference 24.

Finally, to complete the treatment, we include a brief description and numerical results for a steady viscoelastic flow problem following our earlier study in Reference 25. More specifically, we consider the stationary flow of an upper-convected Maxwell fluid as described by (19) and with the constitutive relationship

$$\begin{aligned} \tau_{xx} \left( 1 - 2We \frac{\partial u}{\partial x} \right) + We \left( u \frac{\partial \tau_{xx}}{\partial x} + v \frac{\partial \tau_{xx}}{\partial y} - 2\tau_{xy} \frac{\partial u}{\partial y} \right) - 2 \frac{\partial u}{\partial x} &= 0, \\ \tau_{yy} \left( 1 - 2We \frac{\partial v}{\partial y} \right) + We \left( u \frac{\partial \tau_{yy}}{\partial x} + v \frac{\partial \tau_{yy}}{\partial y} - 2\tau_{xy} \frac{\partial v}{\partial x} \right) - 2 \frac{\partial v}{\partial y} &= 0, \\ We \left( u \frac{\partial \tau_{xy}}{\partial x} + v \frac{\partial \tau_{xy}}{\partial y} - \tau_{xx} \frac{\partial v}{\partial x} - \tau_{yy} \frac{\partial u}{\partial y} \right) + \tau_{xy} - \frac{\partial u}{\partial y} - \frac{\partial v}{\partial x} &= 0, \end{aligned}$$

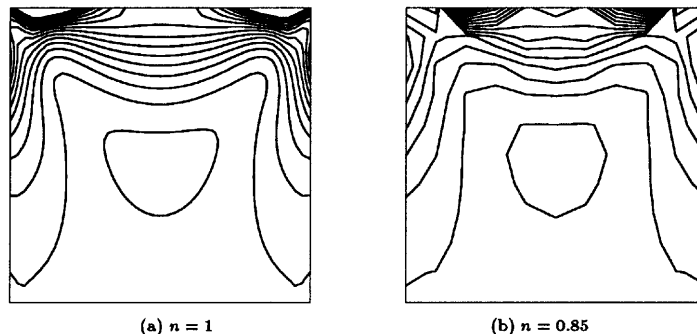


Figure 2. Contours of  $\tau_{xy}$  for lid-driven cavity problem with (a) Newtonian ( $20 \times 20$  mesh of biquadratic elements) and (b) power-law ( $5 \times 5$  mesh of elements with polynomial degree six) fluids



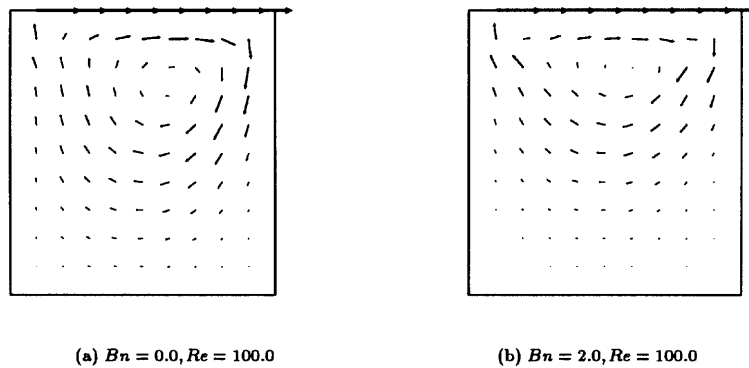


Figure 3. Velocity field for (a) Newtonian and (b) Bingham fluids

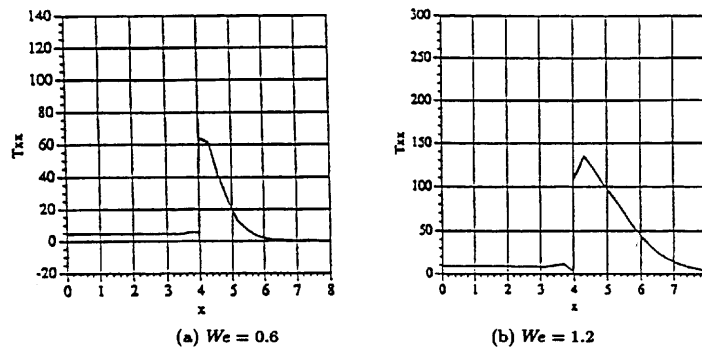


Figure 4. Wall stress distribution

where  $We = \lambda U/L$  is the Weissenberg number. Details of the least-squares system structure are given in Reference 25. Suffice it to say that the system is solved by Newton iteration in conjunction with a line search procedure and incremental continuation in Weissenberg number. As a test case we considered the flow between parallel plates with a fully developed inlet profile at  $x=0$ , stick-slip discontinuity at  $x=4$  and uniform normal stress outflow condition at  $x=64$ . The calculation was made using elements of polynomial degree seven on a mesh that was strongly graded towards the singularity. Results in Figure 4 for the stress component  $\tau_{xx}$  on the wall at  $We=0.6$  and  $1.2$  indicate the pronounced nature of the singularity at the stick-slip point  $x=4$ . We remark here that computations with low-degree elements on moderate meshes have large mass balance errors that are related to the large residuals near the singular point. A graded mesh with high-polynomial-degree elements circumvents this problem. The issue of mass conservation at the stick-slip discontinuity is taken up in a related paper.<sup>26</sup>

## 5. CONCLUDING REMARKS

While there are a growing number of recent studies exploring the least-squares FEM, several important issues concerning questions related to scaling, the use of different forms of the equations, weighting residual contributions for corresponding norms and the effect of  $h$ - or  $p$ -refinement warrant further study. The effect of weighting the terms using a mesh-dependent factor is considered in

Reference 27 but is not conclusive. Related ideas involving the use of an  $H^{-1}$  norm are also being studied.<sup>28</sup> There have also been a number of numerical studies including those in References 21 and 29 for viscous flows, but none of these answers the points raised above or gives as comprehensive a set of studies involving the formulations as we provide here. We remark that we have also considered the time-dependent problem for both wave propagation<sup>30,31</sup> and flow,<sup>32,33</sup> but for brevity have not included any of this work in the present study. In closing, we remark that little has yet been done with respect to the development of adaptive least-squares methods with residual-based error indicators (see References 17 and 34 for work in this direction).

#### ACKNOWLEDGEMENTS

This research has been supported in part by NASA and NSF.

#### REFERENCES

1. B. A. Finlayson, *The Method of Weighted Residuals and Variational Principles*, Academic, New York, 1972.
2. O. C. Zienkiewicz, D. R. J. Owen and K. N. Lee, 'Least-square finite element for elasto-static problems. Use of "reduced" integration', *Int. j. numer. methods eng.*, **8**, 341–358 (1974).
3. G. F. Carey, Y. K. Cheung and S. L. Lau, 'Mixed operator problems using least-squares finite element collocation', *Comput. Methods Appl. Mech. Eng.*, **22**, 121–130 (1980).
4. G. J. Fix and M. D. Gunzburger, 'On least-squares approximation to indefinite problems of mixed type', *Int. j. numer. methods eng.*, **12**, 453–469 (1978).
5. A. I. Pehlivanov, G. F. Carey and R. D. Lazarov, 'Least-squares mixed finite elements for second order elliptic problems', *SIAM J. Numer. Anal.*, **31**, 1368–1377 (1994).
6. G. F. Carey, A. I. Pehlivanov and P. S. Vassilevski, 'Least-squares mixed finite element methods for non-selfadjoint elliptic problems: II. Performance of block-ILU factorization methods', *SIAM J. Sci. Comput.*, **16**, 1126–1136 (1995).
7. J. W. Neuberger, 'Constructive variational methods for differential equations', *Nonlin. Anal.*, **13**, 413–428 (1988).
8. J. W. Neuberger, 'Calculation of sharp shocks using Sobolev gradients', *Contemp. Math.*, **108**, 111–118 (1990).
9. A. I. Pehlivanov, G. F. Carey, R. D. Lazarov and Y. Shen, 'Convergence analysis of least-squares mixed finite elements', *Computing*, **51**, 111–123 (1993).
10. G. F. Carey and Y. Shen, 'Convergence studies of least-squares finite elements for first-order systems', *Commun. Appl. Numer. Methods*, **5**, 427–434 (1989).
11. A. I. Pehlivanov, G. F. Carey and P. S. Vassilevski, 'Least-squares mixed finite element methods for non-selfadjoint elliptic problems: I. Error estimates', *Numer. Math.*, **72**, 501–522 (1996).
12. Z. Cai, R. D. Lazarov, T. A. Manteuffel and S. F. McCormick, 'First order system least squares for second-order partial differential equations: Part I', *SIAM J. Numer. Anal.*, **31**, 1785–1799 (1994).
13. A. I. Pehlivanov and G. F. Carey, 'Error estimates for least-squares mixed finite elements', *RAIRO Math. Model. Numer. Anal.*, **28**, 499–516 (1994).
14. T. F. Chan and P. S. Vassilevski, 'A framework for block-ILU factorizations using block size reduction', *Math. Comput.*, **64**, 129–156 (1995).
15. A. I. Pehlivanov and G. F. Carey, 'Least-squares mixed finite element methods for steady diffusion problems', in G. F. Carey (ed.), *Finite Element Modeling of Environmental Problems*, Wiley, New York, 1995, pp. 287–302.
16. A. I. Pehlivanov and G. F. Carey, 'Interior error estimates for least-squares mixed finite element methods', in preparation.
17. A. I. Pehlivanov and G. F. Carey, 'Least-squares error estimators', in preparation.
18. G. F. Carey and J. T. Oden, *Finite Elements: Fluid Mechanics*, Vol. VI, Prentice-Hall, Englewood Cliffs, NJ, 1986.
19. Y. Shen, 'Least-squares finite element solution and mixing simulation', *Ph.D. Dissertation*, University of Texas at Austin, 1993.
20. G. F. Carey, Y. Shen, A. I. Pehlivanov and A. Bose, *TICAM Rep.*, in preparation.
21. B. N. Jiang and C. L. Chang, 'Least-squares finite elements for the Stokes problem', *Comput. Methods Appl. Mech. Eng.*, **78**, 297–317 (1990).
22. B. N. Jiang and L. A. Povinelli, 'Least-squares finite element methods for fluid dynamics', *Comput. Methods Appl. Mech. Eng.*, **81**, 13–37 (1990).
23. M. J. Crochet, A. R. Davies and K. Walters, *Numerical Simulation of Non-Newtonian Flow*, Elsevier, Amsterdam, 1984.
24. A. Bose and G. F. Carey, 'A least-squares finite element method for Bingham fluids', in preparation.
25. K. C. Wang and G. F. Carey, 'Least-squares finite element method for viscoelastic fluid flow problems', *Int. j. numer. methods in fluids*, **17**, 943–953 (1993).
26. A. Bose and G. F. Carey, 'Issues in least-squares finite element method for viscoelastic flows', in preparation.

27. P. B. Bochev and M. D. Gunzburger, 'Analysis of least-squares finite element methods for the Stokes equations', *Math. Comput.*, **63**, 479–506 (1994).
28. J. H. Bramble, R. D. Lazarov and J. E. Pasciak, 'A least-squares approach based on a discrete minus one inner product for first order systems', *Math. Comput.*, **66**, 935–955 (1997).
29. T. F. Chen, 'On least-squares approximations to compressible flow problems', *Numer. Methods Partial Diff. Eqns.*, **2**, 207–228 (1986).
30. G. F. Carey and Y. Shen, 'Approximations of the KdV equation by least squares finite elements', *Comput. Methods Appl. Mech. Eng.*, **93**, 1–11 (1991).
31. G. F. Carey and Y. Shen, 'Least-squares finite element approximations of the Fisher's reaction-diffusion equation', *Numer. Methods Partial Diff. Eqns.*, **11**, 175–186 (1995).
32. G. F. Carey and Y. Shen, 'Simulation of fluid mixing using least-squares finite element and particle tracing', *Int. J. Numer. Methods Heat Fluid Flow*, **5**, 549–573 (1995).
33. B. N. Jiang and G. F. Carey, 'Least-squares finite element methods for the compressible Euler equations', *Int. j. numer. methods fluids*, **10**, 557–568 (1990).
34. B. N. Jiang and G. F. Carey, 'Adaptive refinement for least square finite elements with element-by-element conjugate gradient solution', *Int. j. numer. methods eng.*, **24**, 569–580 (1987).